11th World Congress on Computational Mechanics (WCCM XI)
5th European Conference on Computational Mechanics (ECCM V)
6th European Conference on Computational Fluid Dynamics (ECFD VI)
E. Oñate, J. Oliver and A. Huerta (Eds)

PREDICTIVE SIMULATIONS FOR PROBLEMS WITH SOLUTION NON-UNIQUENESS

POOJA RAO*, JEREMY A. MELVIN*, WENLIN HU*, RYAN KAUFMAN*, HYUNKYUNG LIM*, DAVID H. SHARP†, JAMES G. GLIMM*

* Stony Brook University
Stony Brook, NY 11794, USA
e-mail: glimm@ams.sunysb.edu, web page: http://www.ams.sunysb.edu

† Los Alamos National Laboratory
Los Alamos NM 87545, USA

Key words: Large Eddy Simulations, Subgrid Scale Models, Front Tracking, Renormalization Group

Abstract. We present our main conclusions regarding the simulation of turbulent mixing, with a summary of previous results and the inclusion of new evidence in support of these conclusions.

Our main conclusions are:

1. Turbulent simulations in the Large Eddy Simulation (LES) regime are inherently non-unique, and require experimental validation before they can be used for scientific or engineering purposes.

2. The level of non-uniqueness is mesh dependent, decreasing to zero as the mesh is refined. The rate of decrease is slow and governed by Kolmogorov exponents when in a scaling regime.

3. Simulation uncertainty is greatly reduced by the use of subgrid scale (SGS) models. For mixing problems (in the case of small time scales or small diffusion parameters), tracking of discontinuities or steep gradients is also essential.

4. Simulation codes have implicitly defined subgrid scale terms within them; each new code or code revision needs its own validation study. For the same reason, higher order subgrid terms, or even summing the missing parts of the Kolmogorov spectrum to reconstruct more exact subgrid terms is not a panacea, and validation (adjustment) of subgrid models is still needed. Within our own validation experiments, we find that low order SGS terms, second order differencing and front tracking (to

control excess diffusion) result, basically, in a perfect fit to experimental data. That is, no further tuning is required for this algorithm.

5. Experimental validation (essential) can be performed at a high but experimentally feasible Reynolds number (Re), followed by an extrapolation to Reynolds numbers needed for engineering design or scientific studies.

6. Convergence of the cumulative distribution functions (CDFs) is important for reactive chemistry coupled to turbulent mixing. We provide a mathematical framework for this convergence, and show that it does occur, with slow rates influenced by Kolmogorov exponents.

Engineering simulations are often regarded as interpolative, not predictive, in their dependence on experimental data. Our conclusions both support this view and indicate a mitigation strategy based on mesh refinement and the appropriate choice of numerical methods.

1 INTRODUCTION

Non-uniqueness for Large Eddy Simulations (LES) of turbulence mixing has been observed in benchmark comparison studies. The non-uniqueness is associated with variations in the choise of numerical algorithms and subgrid scale (SGS) models, which together emulate the influence of unresolved subgrid phenomena. We resolve this issue with a front tracking/LES (FT/LES) algorithm which duplicates experimental values, for predictions of the overall extent of the mixing zone. The experimental validation set is limited to Re = 35,000, and extrapolation methods are presented for verification of turbulent mixing simulations at higher Reynolds numbers.

Issues of reactive chemistry depend on accuracy of solutions at the molecular level, that is, convergence of the probability density functions (PDFs) or their integrals, the cumulative distribution functions (CDFs). CDF convergence raises accuracy issues far more demanding than the size of the mixing zone. A new notion of convergence, based on coarse-graining of solution values and binning (not averaging) the resulting multiple solution values in a single supercell allows convergence of solution CDFs or PDFs. The convergence is observed in the L_1 norm of the associated CDFs.

Convergence of grid level CDFs to an accurate description of molecular level CDFs depends on scaling laws for turbulence phenomena, the most fundamental of which is the Kolmogorov 1941 law. We have begun a verification and validation/uncertainty quantification (V&V/UQ) analysis of CDFs, with convergence studies and studies of sensitivity in dependence on parameters with error bounds, both within experimental regimes and with extrapolation beyond these limits.

Slow convergence rates for the CDFs leads to requirements for extreme levels of simulation mesh refinement. Various mathematical theories, such as Young measures, w*

convergence, scaling laws, the renormalization group (RNG), mathematical existence theories and analysis of SGS terms are used in our analysis. In view of the solution sensitivity to algorithms and to the choice of SGS terms, validation (comparison to experiment) is important to control solution non-uniqueness, and to provide a limit on the valid range of extrapolation outside of experimental data. Stochastic (PDF/CDF) convergence extends to non-linear functionals of the solution, including chemical and nuclear reaction rates, thereby reducing the role of models (which otherwise substitute an approximation to such processes). Such simulations are known as finite rate chemistry in computational chemistry. Models are a major contribution to simulation uncertainty, so that a reduction in their role will improve the simulation reliability. Diagnostic chemical and radiological traces also fall into this category, and their reaction signals, depending on fluctuations and PDFs, are enhanced by convergence issues addressed here.

Mathematical convergence in a strong L_p norm of solutions of the Euler equation was established [1], assuming the Kolmogorov 1941 spectrum bounds [2], in effect a fractional order Sobolev inequality. The proof is by compactness and convergent subsequences, for the incompressible Euler equation, in the limit of vanishing viscosity. From this fact, we conclude that the numerically observed CDF convergence is weaker than optimal. But it is still convenient, and more easily established. Since it extends directly to convergence of nonlinear functionals of the solution, it is directly useful in turbulent reactive flow applications.

2 LES NON-UNIQUENESS

Large Eddy Simulations (LES) are defined by a grid spacing Δx within the inertial range, or equivalently, by $\kappa << \Delta x$, with κ the Kolmogorov scale. In this regime, viscosity plays a small role, so the simulation is effectively conducted at a Reynolds number $Re = \infty$. This choice of Re eliminates one dimensionless parameter from the fluid equations. With the single exception of incompressible single fluid constant density flow, other dimensionless parameters remain and contribute to non-uniqueness, a central point of [3]. This reference links the RNG, LES simulations and the selection of SGS terms, and especially their coefficients. The standard RNG construction is modified for use with LES, in that the remap step is removed and the RNG construction occurs at successively smaller length scales. We identify the choice of SGS and especially the choice of the SGS coefficients, with the RNG step of setting the coefficients of the essential variables to their required values. In contrast with standard RNG, wherein this choice is provided externally to the theory by appeal to experimental values, the dynamic choice of SGS terms is defined (uniquely) by theory, [4, 5, 6] leading to a closed set of SGS equations.

Since this choice has some residual mesh dependence and because the numerical algorithm has some (not modelled) SGS effect on the solution, this unique specification of the equations need not be perfect. Thus, the SGS approach reduces the turbulence error and non-uniqueness, but does not remove it completely, and validation is still an essential

Table 1: Comparison of Rayleigh-Taylor simulation using FT [10, 11, 8] to experiment [12, 13, 14]. The comparison is based on the dimensionless growth rate α of the size of the mixing zone.

Exp.	α_{exp}	α_{sim}
salt-fresh	0.052	0.055
pentane-SF_6	0.072	0.076 ± 0.004
air-He	0.065-0.07	0.069
hot-cold	0.070 ± 0.011	0.075
salt-fresh	0.085 ± 0.005	0.084

part of the scientific simulation. At the validation step, an algorithm specific tuning of the SGS term coefficients should be undertaken.

Evidence for non-uniqueness comes from a benchmark study of the Rayleigh-Taylor instability, (gravity accelerated fluid instabilty) [7], in which some ten codes ran the identical problem, with overall instability growth rates varying by 50% across this suite of codes, and with the ensemble of growth rates different from a large range of laboratory studies by factors of 2 to 3. The explanation cited for this discrepancy is that the experimental data contains unmeasured long wave perturbations. Not only does this explanation fail to account for the code to code variation observed, but we showed [8] (by reconstruction of long wave length perturbations from measured early time data) that long wave length effect is small, with a maximum 10% effect on the overall mixing zone growth rate α. Thus the discrepancy is not explained by long wave length perturbations in the initial data. We suggest the alternate explanation: inappropriate algorithms, lacking both SGS terms and front tracking. To support this conjecture, we present our own study of similar problems, with agreement to experiment, sufficient to distinguish between multiple experiments, each with their own choice of transport coefficients. See Table 1.

In our own work, non-uniqueness of LES simulations and the implications of this fact for engineering practice have been emphasized over the last several years, see [3, 9] for example. Direct numerical evidence of non-uniqueness was demonstrated within a spherical shock induced mixing (Richtmyer-Meshkov) study, as shown in [9]. In this study, we adjust the coefficient of the SGS term governing concentration diffusion up and down by factors of 10. Clear differences in the joint temperature-concentration PDFs were observed, indicating that modification of the SGS coefficients changes the solution.

Comparison of Table 1 with [7] shows reduction of a simulation to experiment discrepancy by nearly two orders of magnitude. To compensate for such serious errors, engineering physics simulations typically employ tuning parameters, set to reproduce experimental values, in the present case, tuning the amplitude of the long wave noise in the initial conditions. From this point of view, we eliminate unphysical values from a tuning parameter, and we eliminate the tuning altogether, so that the FT/LES simulation is predictive, not interpolative. The tuning of the simulation with unphysical input surely

introduces other errors, not diagnosed at this time.

3 MESH DEPENDENCE OF THE SGS COEFFICIENTS

Turbulent convergence rates are governed by scaling law exponents, and are slow in comparison to most non-turbulent fluid simulations. For practical simulations at fine mesh, we thus turn to 2D simulations. Here lies a further complication. The scaling laws [15, 16] are two-fold, with a $k^{-5/3}$ turbulent kinetic energy scaling at wave numbers $\lambda \geq \lambda_c$ and k^{-3} for smaller values of λ. The transition between the two scaling exponents, λ_c, is equal to the wave number of the input causing the turbulent flow.

For the reshocked Richtmyer-Meshkov study [17], the reshock introduces small length scales only slightly larger than Δx, and so the $k^{-5/3}$ scaling law is observed. We study the SGS terms, scaled by this exponent, and find that they are nearly independent of mesh size. See Table 2, taken from [17]. An approximate uniformity under mesh refinement is observed from comparison of rows I, II, III.

4 STOCHASTIC CONVERGENCE OF CDFs

4.1 The conceptual framework

Stochastic convergence is realized in a post processing manner starting from a normal grid based simulation. The basic idea of stochastic convergence is to partition the simulation information between the geometrical or space-time resolution and statistical resolution of the stochastic state space variables (momentum, density, temperature, concentration). The partition is achieved by use of a coarse grid, each cell of which is called a supercell. Each supercell is a union of a number of mesh cells. The space-time geometrical information is realized relative to the coarse grid only. Within a single supercell, we disregard the spatial-temporal information, and consider the ensemble of state values as a finite approximation to the solution probability density function (PDF) at the space time location of the supercell. These general concepts are explained in [18, 19].

Based on this supercell picture, we compare two solutions, using the L_1 norm of the difference of the CDFs in each supercell, then an L_1 norm of this supercell norm difference, integrated over supercells, to obtain a norm measuring the difference between the solutions [20, 9, 21]. We apply this norm to measure mesh convergence as well as the effect of parameter variation. This stochastic comparison is also relevant to the comparison of simulation to experimental or observational data or the comparison of experimental or observational data sets to one another.

A software tool W* has been constructed to carry out this norm comparison. Numerical evidence of convergence has been presented for a series of turbulent mixing problems, together with further analysis of this concept [19]. The tool can be accessed at:

http://www.ams.sunysb.edu/wstar

Table 2: Scaled mean turbulent transport coefficients for a cylindrically symmetric Richtmyer-Meshkov implosion. Mesh I is 400×800; mesh II has double the resolution and mesh III is doubled again. The time is shortly after the passage of reshock. Comparison of mesh levels I, II, III shows variation in the range of $\pm 10\%$, while comparison along individual rows shows a similar level of parameter dependence in the $Re = \infty$ limit. The same comparison, of the extreme ends of each row illustrates the small effects that result from Re variation within this range. Here ν^a_{turb}, ν^i_{turb}, μ_{turb} and α_{turb} denote the coefficients of anisotropic and isotropic turbulent diffusion, of turbulent concentration diffusion and of turbulent thermal heat conduction, respectively.

Mesh	$Re = 3.5 \times 10^4$	$Re = 6 \times 10^5$	$Re = 6 \times 10^6$	$Re = 6 \times 10^7$	$Re = \infty$
$\nu^a_{\rm turb}/\Delta x^{4/3}$ = scaled anisotropic turbulent viscosity ($\rm m^{2/3}/sec$)					
I	44	51	53	47	54
II	48	48	56	58	53
III	57	49	64	64	62
$\nu^i_{\rm turb}/\Delta x^{4/3}$ = scaled isotropic turbulent viscosity ($\rm m^{2/3}/sec$)					
I	214	248	238	214	234
II	222	236	234	232	235
III	253	233	276	277	260
$\mu_{\rm turb}/\Delta x^{4/3}$ = scaled species turbulent diffusion ($\rm m^{2/3}/sec$)					
I	112	136	127	127	124
II	115	133	128	122	124
III	133	122	149	148	133
$\alpha_{\rm turb}/\Delta x^{4/3}$ = scaled turbulent thermal diffusion ($\rm m^{2/3}/sec$)					
I	126	163	143	122	132
II	106	181	158	135	145
III	103	174	191	174	149

4.2 Numerical convergence: verification

The mesh convergence of CDFs, PDFs and second moments has been reported in our earlier publications [9, 22], in studies of a circular Richtmyer-Meshkov implosion and in [21], in simulations of planar Rayleigh-Taylor instability. Joint temperature-concentration CDFs were analyzed in [9, 22]. Ref. [22] considered fluids with parameters suggestive of gases, liquids and plasmas, while [9] considered plasma-like fluids only. The plasma like fluids are characterized by a high level of thermal conductivity (small Prandtl number). For the plasma like fluids, we observed a convergence rate of about 1/2 under mesh refinement, over a range of Re values, for a cylindrical Richtmyer-Meshkov implosion. To the extent that convergence is limited by turbulent fluctuations, spectral analysis would predict a convergence order somewhat worse than 1/3. Probably the use of CDFs to measure convergence is related to the higher rate actually observed. For transport parameters typical of liquids and gases, somewhat better convergence was observed.

In Fig. 1, we plot the L_1 norm of convergence errors in the concentration CDFs at

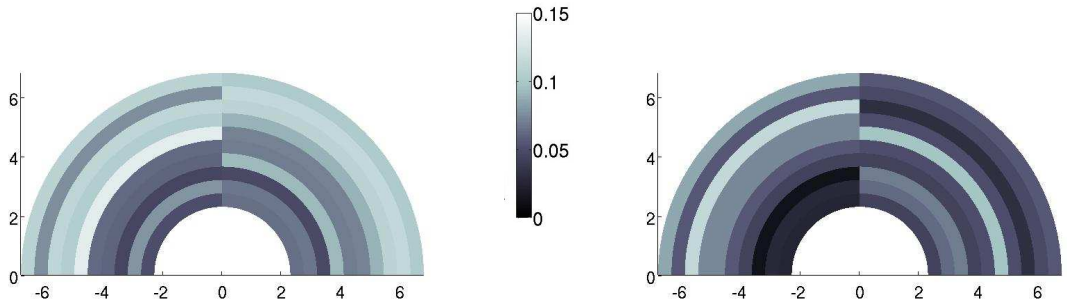

Figure 1: Mesh convergence of the concentration CDFs is demonstrated visually, with data from [9]. The left frame compares the coarse to fine mesh; the right frame compares the medium to fine mesh. Colors indicate the level of CDF mesh error in each supercell. Expressing this convergence as an L_1 norm, the order of convergence is 1/2.

$Re = 6 \times 10^7$. The picture represents a time after reshock. The turbulence is developed at this time and the high values of Re are reflective of the Kolmogorov hypothesis. In the left frame, the coarse grid is compared with the fine grid and in the right frame, the medium grid is compared with the fine grid. The order of the mesh convergence, using L_1 norm, is about 1/2, which is slightly better than order of convergence of joint concentration-temperature CDFs [9]. The low order of convergence in the latter case is speculated to be due to Kolmogorov scaling.

The Rayleigh-Taylor simulation study [21] shows mesh convergence of second moments of concentration. CDF convergence of the fluid concentration was demonstrated, using the W* software tool. The convergence was seen to depend on the supercell size, with convergence improving as the supercell size is increased.

4.3 Comparison to experiment: validation

We model the hot-cold and fresh-salt water channels of [23]. The second moment θ of the fluid mixing is recorded experimentally, as a function of time, with experimental error bars. We show in Fig. 2, the hot-cold water channel experimental measured values of [23], together with three simulations: an incompressible (nearly) DNS simulation [23], a compressible front tracking simulation from [20] and an incompressible front tracking simulation, newly reported here. We also show a similar comparison between the experiment and the FT simulation for the fresh-salt water mixing. This flow has a high Schmidt number, $Sc = 560$, and is accessible only to a tracked simulation.

From both data sets, we see validation of the FT/LES simulation. For the hot-cold water experiment, we see the improvement offered by Front Tracking, even in comparison to a nominally DNS simulation.

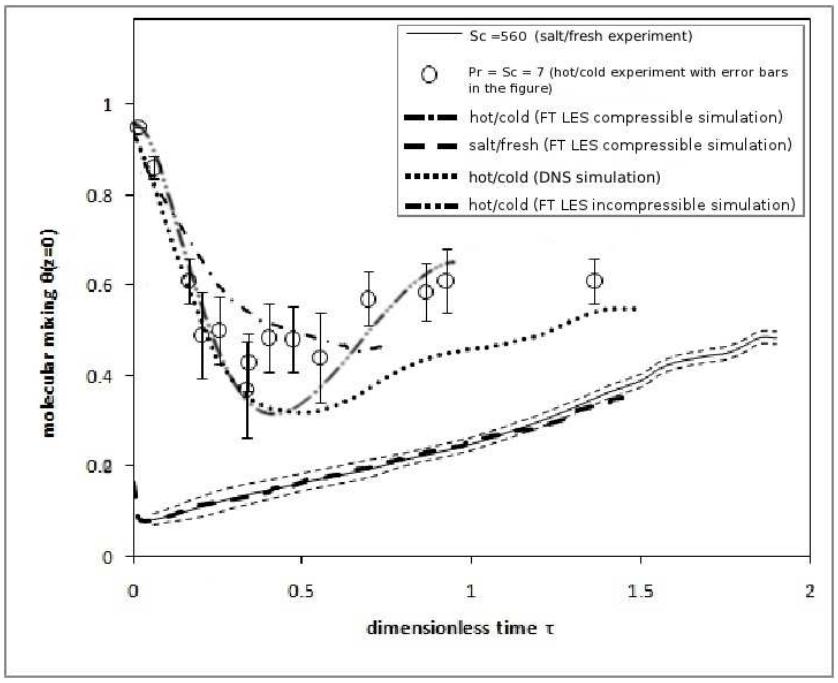

Figure 2: Hot-cold water channel splitter plate experiment of Rayleigh-Taylor instability with experimental measurements [23], the nearly DNS incompressible simulation, our own front tracking incompressible simulation using lower grid resolution, a compressible front tracking simulation reported earlier [20] and fresh-salt water channel experiments and simulations. The very large Schmidt number $Sc = 560$ makes this case infeasible to simulate without the use of front tracking.

5 FINITE Re APPROXIMATION TO $Re = \infty$

Our main result is the near equivalence of the SGS coefficients under change of Re, within the range $35,000 \leq Re \leq \infty$, which links experimental validation to high Re applications. We refer to Table 2, and compare the first and last entries (or all the entries) on a single row, at the finest mesh III. The variation is 10%, with the exception of the thermal SGS terms.

The thermal field for the reshocked circular Richtmyer-Meshkov instability with plasma-like fluid parameters has a very high laminar (molecular) thermal diffusivity, with a Prandtl number $Pr = 10^{-4}$. This high thermal conductivity, in a true plasma, results from the coupling of the ions to the electrons. The later, being light, have a very high thermal conductivity. As a result, the thermal properties do not see a high Re flow, in that the laminar thermal conductivity dominates the turbulent thermal conductivity for finite Re, even up to $Re = 6 \times 10^7$.

To explain this effect more clearly, we tabulate the turbulent coefficients as a fraction of the total (turbulent plus laminar) transport, see Table 3. We observe clearly the rapid convergence of total transport for all coefficients, with the exception of the Prantdl

Table 3: Values of the turbulent transport coefficients as a fraction of total transport, turbulent / total; total = laminar + turbulent, for a circular Richtmyer-Meshkov instability after reshock, raw data from [17], using the finest mesh (III). The laminar isotropic viscosity coefficient was set to zero, so that the fractional turbulent coefficient is 1 for all values of Re.

Frac. turb. coef.	$Re = 3.5 \times 10^4$	$Re = 6 \times 10^5$	$Re = 6 \times 10^6$	$Re = 6 \times 10^7$	$Re = \infty$
Anisotropic visc.	0.35	0.89	0.99	1.00	1.00
Isotropic visc.	1.00	1.00	1.00	1.00	1.00
Species diff.	0.56	0.95	1.00	1.00	1.00
Thermal diff.	0.00	0.01	0.05	0.34	1.00

number, which even at the highest finite value of Re considered, still has significant finite Re effects.

6 CONCLUSIONS

Engineers and applied physicists often insist that their codes are suitable for interpolation, but fail to be scientifically predictive when used outside the range of validating experimental data. In this paper,

- we have traced one aspect of this shortcoming to essential and fundamental aspects of turbulence.

- we suggest mitigating strategies: Use of dynamic SGS terms in an LES framework, and if steep gradients or discontinuities are present, use of front tracking. These steps appear to reduce the mesh errors in a problem dependent manner. For one problem with fully developed turbulence and a strong dependence on fluid transport parameters (Rayleigh-Taylor mixing), the improvement is dramatic. This (improved) code still needs validation, a step which is typically possible only at the "wrong" value of Re. But if the validating Re is high enough, the extrapolation to larger Re might be mild, for which a mesh based (verification) study might suffice.

- we present evidence for convergence of the CDFs, with further studies still to be conducted. The convergence of the CDFs allows the computation of chemical or nuclear reactions without the use of combustion models, thereby reducing a significant uncertainty in the compuation of turbulent reactive flows.

7 ACKNOWLEDGEMENTS

This reserch was supported in part by Leland Stanford Junior University (subaward with DOE as prime sponsor), the Army Research Office W911NF-13-1-0249 and LANL award JLKDONYSB0000. This research used resources of the Argonne Leadership Computing Facility at Argonne National Laboratory, which is supported by the Office of Sci-

ence of the U.S. Department of Energy under contract DE-AC02-06CH11357. Preprint, Los Alamos National Laboratory LA-UR-14-21546.

REFERENCES

[1] Chen, G.-Q. and Glimm, J. (2012) Kolmogorov's theory of turbulence and inviscid limit of the Navier-Stokes equations in R^3. *Commun. Math. Phys.*, **310**, 267–283.

[2] Kolmogorov, A. N. (1941) Local structure of turbulence in incompressible viscous fluid for very large Reynolds number. *Doklady Akad. Nauk. SSSR*, **30**, 299–3031.

[3] Glimm, J., Plohr, B., and Sharp, D. (2013) Large Eddy Simulation, Turbulent Transport And The Renormalization Group. arXiv:1308.3221, Los Alamos National Laboratory Preprint Number LA-UR-12-26149, Stony Brook University Preprint Number SUNYSB-AMS-12-02.

[4] Germano, M., Piomelli, U., Moin, P., and Cabot, W. H. (1991) A dynamic subgrid scale eddy viscosity model. *Phys. Fluids A*, **3**, 1760–1765.

[5] Moin, P., Squires, K., Cabot, W., and Lee, S. (1991) A dynamic subgrid-scale model for compressible turbulence and scalar transport. *Phys. Fluids A*, **3**, 2746–2757.

[6] Ma, T. (2006) *Large eddy simulation of variable density flows*. Ph.D. thesis, University of Maryland.

[7] Dimonte, G., et al. (2004) A comparative study of the turbulent Rayleigh-Taylor instability using high-resolution three-dimensional numerical simulations: The Alpha-Group collaboration. *Phys. Fluids*, **16**, 1668–1693.

[8] Glimm, J., Sharp, D. H., Kaman, T., and Lim, H. (2013) New directions for Rayleigh-Taylor mixing. *Phil. Trans. R. Soc. A*, **371**, 20120183, Los Alamos National Laboratory Preprint LA-UR 11-00423 and Stony Brook University Preprint SUNYSB-AMS-11-01.

[9] Melvin, J., Rao, P., Kaufman, R., Lim, H., Yu, Y., Glimm, J., and Sharp, D. H. (2013) Atomic scale mixing for inertial confinement fusion associated hydro instabilities. *High Energy Density Physics*, **9**, 288–298, Stony Brook University Preprint SUNYSB-AMS-12-01 and Los Alamos National Laboratory Preprint LA-UR 12-21555.

[10] Liu, X.-F., George, E., Bo, W., and Glimm, J. (2006) Turbulent mixing with physical mass diffusion. *Phys. Rev. E*, **73**, 056301.

[11] Lim, H., Iwerks, J., Glimm, J., and Sharp, D. H. (2010) Nonideal Rayleigh-Taylor mixing. *Proc. Nat. Acad. Sci.*, **107(29)**, 12786–12792, Stony Brook University

Preprint SUNYSB-AMS-09-05 and Los Alamos National Laboratory Preprint LA-UR 09-06333.

[12] Smeeton, V. S. and Youngs, D. L. (1987) Experimental investigation of turbulent mixing by Rayleigh-Taylor instability (part 3). AWE Report Number 0 35/87.

[13] Ramaprabhu, P. and Andrews, M. (2004) Experimental investigation of Rayleigh-Taylor mixing at small atwood numbers. *J. Fluid Mech.*, **502**, 233–271.

[14] Mueschke, N. J. (2008) *Experimental and numerical study of molecular mixing dynamics in Rayleigh-Taylor unstable flows*. Ph.D. thesis, Texas A and M University.

[15] Kraichnan, R. H. (1967) Inertial ranges in two-dimensional turbulence. *J. Fluid Mech.*, **16**, 1417–1423.

[16] Boffetta, G. (2007) Energy and enstrophy fluxes in the double cascade of two-diemnsional turbulence. *J. Fluid Mech*, **589**, 253–260.

[17] Melvin, J., Rao, P., Kaufman, R., Lim, H., Yu, Y., Glimm, J., and Sharp, D. H. (2013) Turbulent transport at high reynolds numbers in an ICF context. *ASME Journal of Fluids Engineering*, **submitted**.

[18] Melvin, J., Kaufman, R., Lim, H., Kaman, T., Rao, P., and Glimm, J. (2013) Macro and micro issues in turbulent mixing. *Science China Technological Sciences*, pp. 1–6.

[19] Kaufman, R., Kaman, T., Yu, Y., and Glimm, J. (2012) Stochastic convergence and the software tool W*. *Proceeding Book of International Conference to honour Professor E.F. Toro*, pp. 37–41, CRC, Taylor and Francis Group, stony Brook University Preprint number SUNYSB-AMS-11-10.

[20] Lim, H., Kaman, T., Yu, Y., Mahadeo, V., Xu, Y., Zhang, H., Glimm, J., Dutta, S., Sharp, D. H., and Plohr, B. (2012) A mathematical theory for LES convergence. *Acta Mathematica Scientia*, **32**, 237–258, Stony Brook University Preprint SUNYSB-AMS-11-07 and Los Alamos National Laboratory Preprint LA-UR 11-05862.

[21] Kaman, T., Kaufman, R., Glimm, J., and Sharp, D. H. (2012) Uncertainty quantification for turbulent mixing flows: Rayleigh-Taylor instability. Dienstfrey, A. and Boisvert, R. (eds.), *Uncertainty Quantification in Scientific Computing*, vol. 377 of *IFIP Advances in Information and Communication Technology*, pp. 212–225, Springer, stony Brook University Preprint number SUNYSB-AMS-11-08.

[22] Lim, H., Yu, Y., Glimm, J., Li, X. L., and Sharp, D. H. (2010) Subgrid models for mass and thermal diffusion in turbulent mixing. *Physica Scripta*, **T142**, 014062, stony Brook Preprint SUNYSB-AMS-08-07 and Los Alamos National Laboratory Preprint LA-UR 08-07725.

[23] Mueschke, N. and Schilling, O. (2009) Investigation of Rayleigh-Taylor turbulence and mixing using direct numerical simulation with experimentally measured initial conditions. II. Dynamics of transitional flow and mixing statistics. *Physics of Fluids*, **21**, 014107 1–16.